# Study on Sliding Base Isolation System Utilizing High Viscous Liquid with Large Damping Effects

**T. Ito, A. Shintani & C. Nakagawa**
*Mechanical Engineering Graduate Scholl of Engineering Osaka Prefecture University, 1-1 Gakuencho, Naka-ward, Sakai City, Osaka prefecture, Japan*

**SUMMARY:**
For suppressing the sliding motion of very heavy cylindrical structures, the authors developed a sliding motion suppression system utilizing high viscous liquid and coaxial circular cylinders. Coaxial circular cylinders are installed at the bottom end of the cylinder and high viscous liquid is installed in the annular spaces. High viscous liquid in the annular spaces will cause very large added damping effects, thus sliding motion will be expected to be suppressed. In this study, added damping effects of the annular space liquid and sliding motion suppression effects are studied analytically and experimentally using a fundamental test model. It is found that increase in liquid viscosity brings us very large displacement suppression effects, however, at the same time, response acceleration increases which should be reduced in the view point of mitigation of rocking motion and structural integrity of the inner structure. Therefore, it is said that optimization in liquid viscosity will be needed.

## 1. INTRODUCTION

In Japan, spent fuels are planning to be stored in a temporal site before reprocessed at the reprocessing plant. In this site, spent fuels are installed in a cylindrical container called cask-canister system. This system is a free-standing structure, thus is seen as a sliding isolation system. When this system is subjected to strong seismic motions, large sliding motion will be induced. Previous investigations by the authors on the sliding motion of a cask-canister system subjected to a strong seismic excitation showed that, in the worst case, the cask-canister system may collide to each other. Therefore, it is very important to reduce sliding motions of the cask in order to avoid the collision of cask systems and consequent contamination of radio-active substances.

For suppressing the sliding motion, the authors developed a sliding motion suppression system utilizing high viscous liquid and coaxial circular cylinders. Coaxial circular cylinders are installed beneath the cask and high viscous liquid is installed in the annular spaces. High viscous liquid in the annular spaces will cause very large added damping effects, thus sliding motion will be expected to be suppressed

In this study, added damping and sliding displacement suppression effects of the annular space liquid are studied analytically and experimentally. In the analyses, response displacement and acceleration for the actual cask systems are evaluated for various damping coefficients. In the experiments, a coaxial circular cylinder system and a fundamental sliding type base isolation system are fabricated. Using these test apparatuses, the added damping coefficient for various liquid viscosities and diameter ratios are measured. And sinusoidal excitation tests are conducted using shaking table and sliding displacement and response acceleration are measured for various liquid viscosity and diameter ratios.

It is found that increase in liquid viscosity causes very large displacement suppression effects, however, at the same time, response acceleration increases which should be reduced in the view point of mitigation of rocking motion and the structural integrity of the inner structures. Therefore, it is said that optimization in liquid viscosity is needed.

## 2. LIQUID ADDED MASS AND ADDED DAMPING ACTING ON INNER CYLINDER

When we consider a coaxial circular cylinder where viscous liquid is filled in the annular space, Chen formulated added mass and added damping of liquid acting on the cylinders. The equation of motion of liquid in the annular space is derived and solved for the boundary conditions under the assumptions of sinusoidal vibration. Pressure distribution around the inner cylinder can be obtained and by integrating this pressure distribution, liquid force acting on the inner cylinder will be obtained. The liquid force associated to velocity refers to added damping while that associated to acceleration does added mass of liquid. Chen calculated added mass coefficient $C_m$ and added damping coefficient $C_d$ as functions of the diameters of the inner and outer cylinders of $D$ and $d$, vibration circular frequency $\omega$ and kinetic coefficient of viscosity $\nu$, for various diameter ratios $D/d$ and Reynolds number $S$ ($=\omega d^2/\nu$). These results indicate that $C_m$ and $C_d$ show very steep increase when $D/d$ approaches to unity, i.e., when the gap between the inner and outer cylinders becomes zero. We utilize the damping force of high viscous liquid in the annular space of a coaxial circular cylinder in order to suppress displacement of sliding motion.

## 3. SLIDING MOTION ANALYSIS

### 3.1. Analytical Model

Fig. 3.1 illustrates the outline of the sliding base isolation system proposed here. Beneath the upper structure, a high damping device is installed. An inner cylinder is attached at the bottom surface of the upper structure, and composes a coaxial circular cylinder. This high damping device consists of a coaxial circular cylinder, viscous liquid in the annular space and the outer cylinder fixed to the floor. When the upper structure is subjected to seismic excitations, the upper structure will slide at the upper surface of the outer cylinder. In this study, the upper structure is assumed to be a rigid body and treated as a single –degree-of freedom system. The analytical model is shown in Fig. 3.2. Total mass of the upper structure and the inner cylinder is expressed by $m$. Added damping coefficient due to high damping devise is defined by $C_a$. Seismic excitation acceleration is expressed by $a_h$. Seismic excitation displacement, relative displacement and absolute displacement of the upper structure are $x_h$, $x$ and $\xi$, respectively. In this study, vertical excitation is not considered for simplicity.
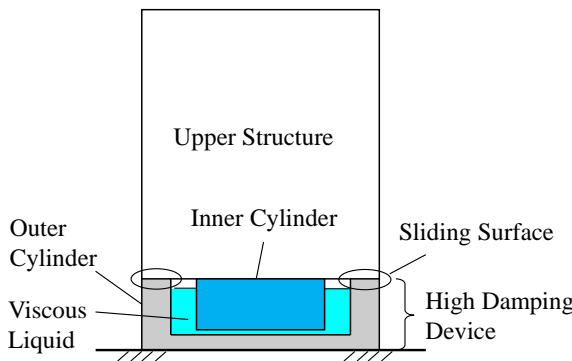


**Fig. 3.1.** Outline of Proposed Base Isolation System          **Fig. 3.2.** Analytical Model
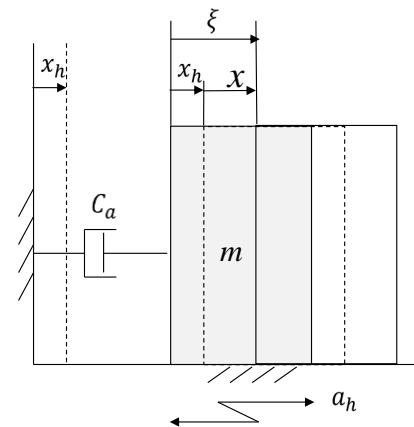
### 3.2. Equation of Motion

The equation of motion for the analytical model shown in Fig. 3.2 is expressed as,

$$(m+m_a)\ddot{\xi} = -f - c_a\dot{x} \tag{3.1}$$

Here, $m_a$ is added mass of viscous liquid in the annular space, and $f$ is friction force acting on the upper structure. The added mass $m_a$ is evaluated based on the following equation proposed by Chen for the

cylinders with infinite length,

$$m_a = \frac{D^2 + d^2}{D^2 - d^2} m_f, \quad m_f = \rho \frac{\pi}{4} d^2 L \quad (3.2)$$

Here, $\rho$ and $L$ are liquid density and immersed length of the inner cylinder, respectively. The absolute displacement $\xi$ and friction force $f$ are expressed as,

$$\xi = x_h + x \quad (3.3)$$

$$f = \mu_k mg \, \text{sgn}(\dot{x}) \quad (3.4)$$

Where, $\mu_k$ is dynamic friction coefficient and $g$ is acceleration of gravity. The onset condition of sliding motion is,

$$|\ddot{x}_h| = |a_h| \geq \mu_s g \quad (3.5)$$

Here, $\mu_s$ is static friction coefficient.

## 3.3. Analytical Condition

In this analysis, the proto type cask-canister system is treated. The dimensions are shown in Table 3.1. Mass of the structure is 187000 kg, and $\mu_s$ and $\mu_k$ are assumed to be 0.5 and 0.2, respectively. As base excitations, sinusoidal excitation and seismic wave excitation are employed. Acceleration of sinusoidal excitation is expressed as,

$$a_h = M_{ah} \sin 2\pi f_{ah} t \quad (3.6)$$

Here, $M_{ah}$ and $f_{ah}$ are acceleration amplitude and excitation frequency, respectively. As for the seismic wave, the recorded wave at Sendai city in the horizontal direction at the Great East Japan Earthquake occurred on March 11 in 2011 is employed. Fig. 3.3 shows the time history and response acceleration spectrum. The predominant frequency is around 4 Hz and the maximum acceleration is 2700 m/s$^2$. In the analyses, sliding response displacement and response acceleration are evaluated for various added damping coefficients. Numerical simulations are conducted using general purpose software MATLAB and solver ode 45.

**Table 3.1.** Dimensions of Analytical Model

| Items | Symbol | Value | Unit |
|---|---|---|---|
| Mass | $M$ | 187000 | kg |
| Static friction coefficient | $\mu_s$ | 0.5 | - |
| Dynamic friction coefficient | $\mu_k$ | 0.2 | - |
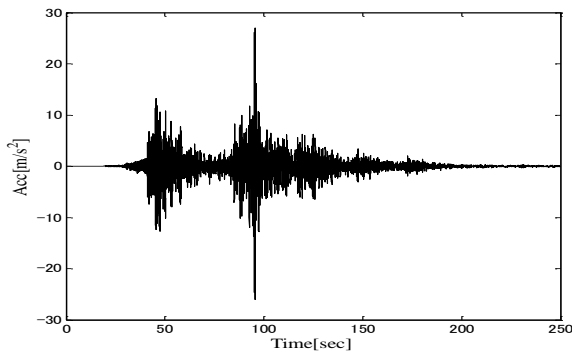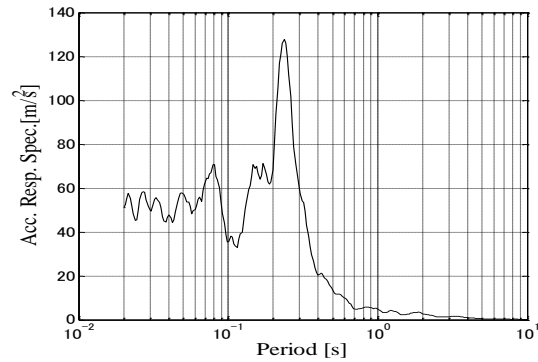


(a) Time history        (b) Response acceleration spectrum
**Fig. 3.3.** Seismic Wave at Sendai City in the Great East Japan Earthquake in 2011

## 3.4. Sliding Response for Sinusoidal Excitation

In order to grasp the effects of added damping, response displacement and acceleration are evaluated for various values of $C_a$, keeping the excitation amplitude and frequency as $M_{ah}$ =5 m/s$^2$, $f_{ah}$=2 Hz. Displacement and acceleration time histories for $C_a$ =0, $10^6$, 4x$10^6$ and 8x$10^6$ Ns/m are shown in Figs.

3.4 and 3.5. In these figures, very large reduction in sliding displacement due to added damping is found, while sliding acceleration increases. Figure 3.6 shows the effects of damping coefficient $C_a$ on maximum sliding response displacement and response acceleration. As well as noted in Figs. 3.4 and 3.5, when we increase added damping coefficient $C_a$, very large sliding displacement suppression is found, while sliding acceleration increases significantly. And this change occurs drastically as $C_a$ exceeds around $10^5$ Ns/m. In order to avoid collision of the casks, displacement should be minimized, but in order to reduce rocking motion or keep structural integrity of the inner structure such as spent fuels, acceleration should be minimized. Therefore, it is said that optimization is needed for $C_a$.
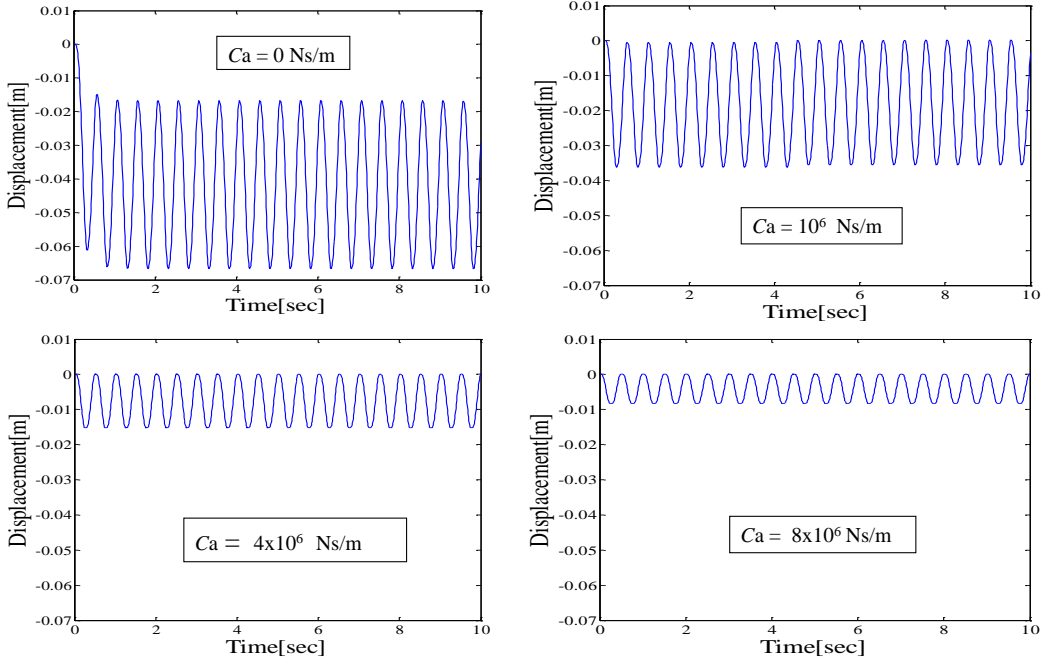


**Fig. 3.4.** Response Displacement Time Histories for Sinusoidal Excitation $(M_{ah}=5$ m/s$^2$, $f_{ah}=2$Hz$)$
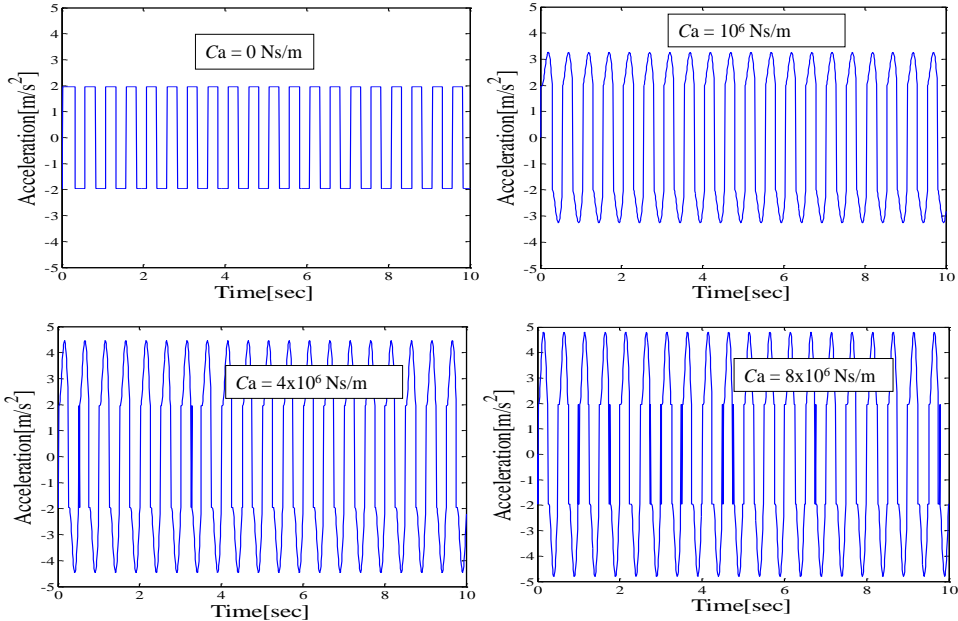


**Fig. 3.5.** Response Acceleration Time Histories for Sinusoidal Excitation $(M_{ah}=5$ m/s$^2$, $f_{ah}=2$Hz$)$
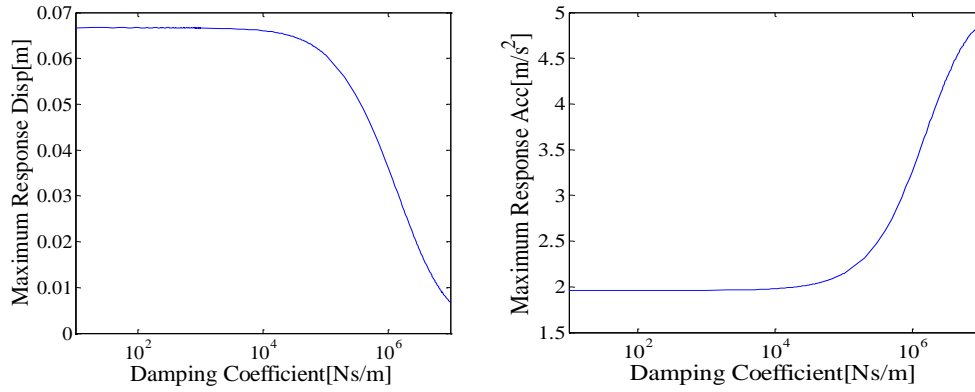
**Fig. 3.6.** Maximum Response Displacement and Acceleration for Various Added Damping Coefficients for Sinusoidal Excitation

## 3.5. Sliding Response for Seismic Excitation

Similar simulations are conducted as those for sinusoidal excitations. Figures 3.7 and 3.8 illustrate the response time histories corresponding to Figs. 3.4 and 3.5, and Fig. 3.9 is the figure corresponding to Fig. 3.6. Similar tendencies are found in the responses for the seismic excitations. Therefore, we should choose optimum damping coefficient.
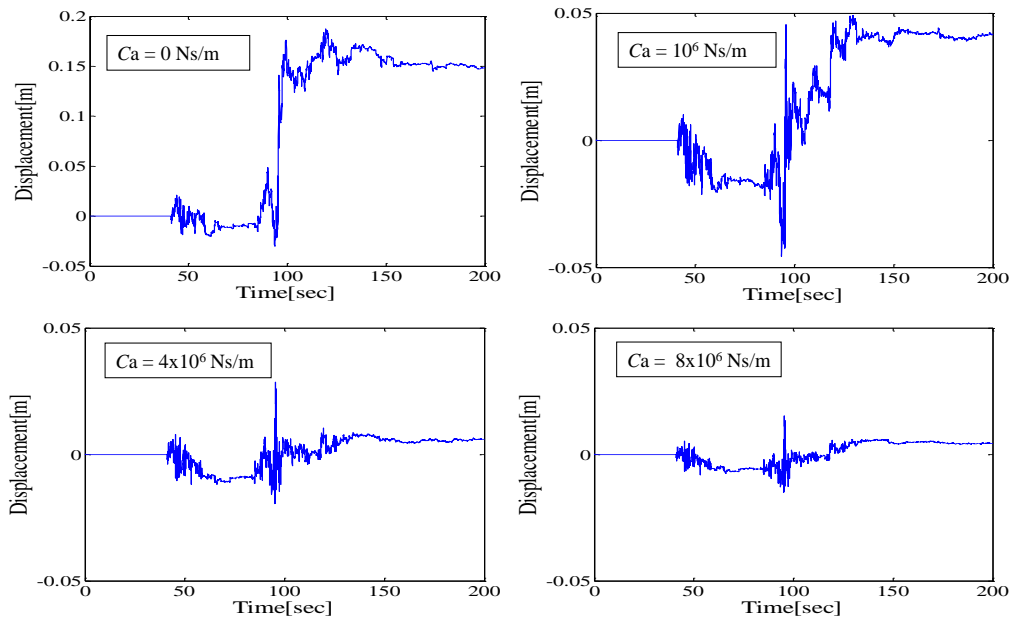


**Fig. 3.7.** Response Displacement Time Histories for the Great East Japan Earthquake

## 4. EXPERIMENT FOR MESURING DAMPING COEFFICIENT

Damping coefficient can be evaluated according to the procedure shown in Chapter 2. However, evaluation accuracy will tend to decrease for coaxial circular cylinders with very small gap. In addition to this, it is better to grasp the relationship between liquid viscosity and damping coefficient experimentally. Thus, fundamental tests are conducted for measuring the damping coefficient.

### 4.1. Experimental Set-up

Simple coaxial circular cylinder is fabricated. Figure 4.1 shows the outline of the test apparatus and the photo. Inner and outer cylinders are made of poly vinyl chloride (PVC) and inner cylinder is supported by two leaf springs from the upper ceiling, thus will vibrate as a single degree-of-freedom system. Only the sway motion is allowed for the inner cylinder. Outer cylinder is fixed to the steel
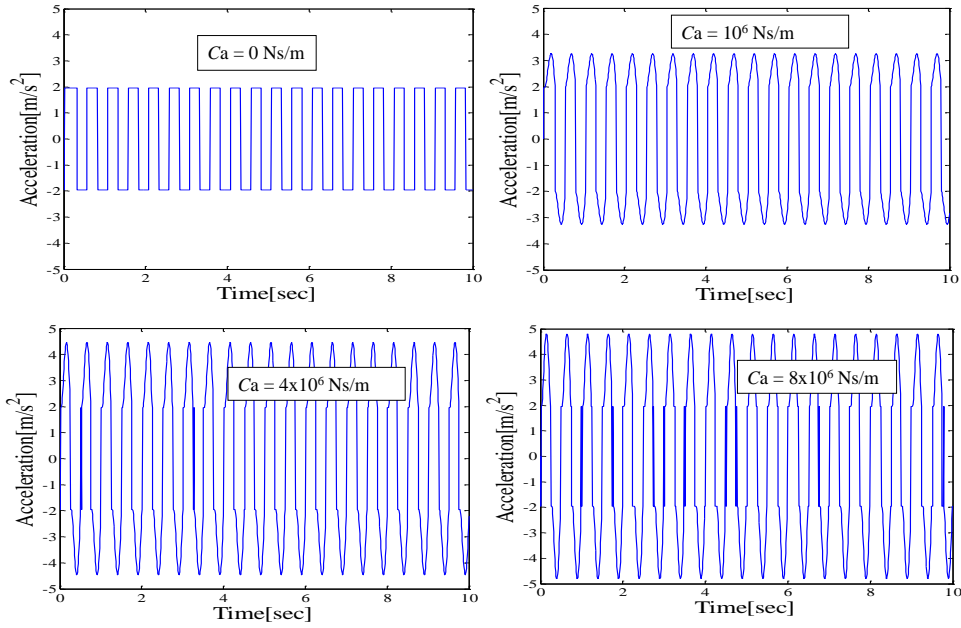
**Fig. 3.8.** Response Acceleration Time Histories for the Great East Japan Earthquake
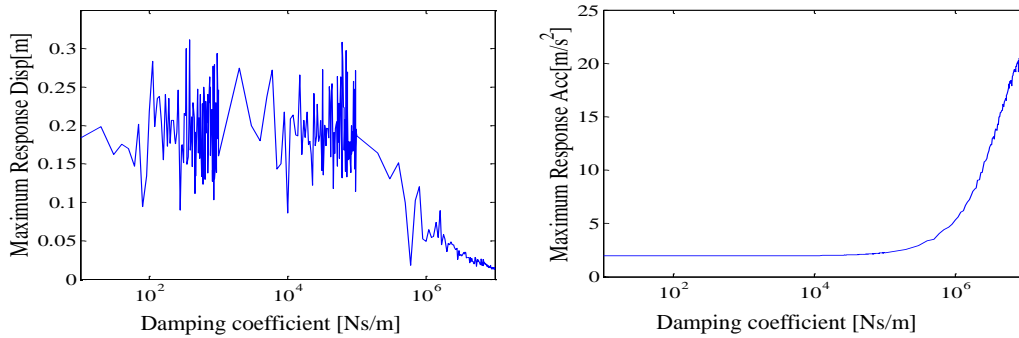


**Fig. 3.9.** Maximum Response Displacement and Acceleration for Various Added Damping Coefficients for the Great East Japan Earthquake

base plate. The inner diameter of the outer cylinder is fixed to 110 mm. 5 kinds of inner cylinders with different outer diameter of 60, 70, 80, 90 and 100 mm are fabricated in order to change the diameter ratio. For these diameters, the gap between the inner and outer cylinders are 5, 10, 15, 20 and 25 mm. Length of the inner cylinder is kept constant as100 mm. Natural frequency of the inner cylinder in air is around 24 Hz. Silicon oil with 5 different viscosity are used. Viscosity is varied from 100 mm$^2$/s to 50000 mm$^2$/s. Table 4.1 summarizes test conditions. Here, case I is the same test as case C.

Vibration displacement of inner cylinder is measured by a laser type displacement transducer. Initial displacement is applied to the inner cylinder and free vibration is measured. From the response time histories, damping ratio is evaluated and from damping ratio, damping coefficient is obtained. Here, for over-damping case, vibration does not occur. Thus damping ratio is deduced by comparing the time histories obtained experimentally and analytically. For these coaxial circular cylinders, added mass of viscous liquid will become very large. Thus, the added mass is evaluated using Eqn. 3.2.

### 4.2. Experimental Results
Time histories of free vibration for case A, C, E and G are shown in Fig. 4.2. In these figures, vary large damping effects are fond due to viscous liquid. Time history for case E is typical one for over-damping case. At first, damped natural frequencies are evaluated from time histories. Damped natural frequencies for case A, B. C, G, H and I are 23.0, 17.5, 16.7 22.0, 19.2 and 15.2 Hz

respectively. Damping ratios are also measured. Using these values, damping coefficients are

**Table 4.1.** Test Conditions for Damping Coefficient Tests

| Case | $d$ (mm) | Radial Gap (mm) | $d/D$ | Kinematic Coefficient of Viscosity (mm$^2$/s) |
|------|----------|-----------------|-------|-----------------------------------------------|
| A | 80 | 15 | 0.73 | 0 |
| B | 80 | 15 | 0.73 | 100 |
| C | 80 | 15 | 0.73 | 1000 |
| D | 80 | 15 | 0.73 | 5000 |
| E | 80 | 15t | 0.73 | 10000 |
| F | 80 | 15 | 0.73 | 50000 |
| G | 60 | 25 | 0.55 | 1000 |
| H | 70 | 20 | 0.64 | 1000 |
| I | 80 | 15 | 0.73 | 1000 |
| J | 90 | 10 | 0.82 | 1000 |
| K | 100 | 5 | 0.91 | 1000 |
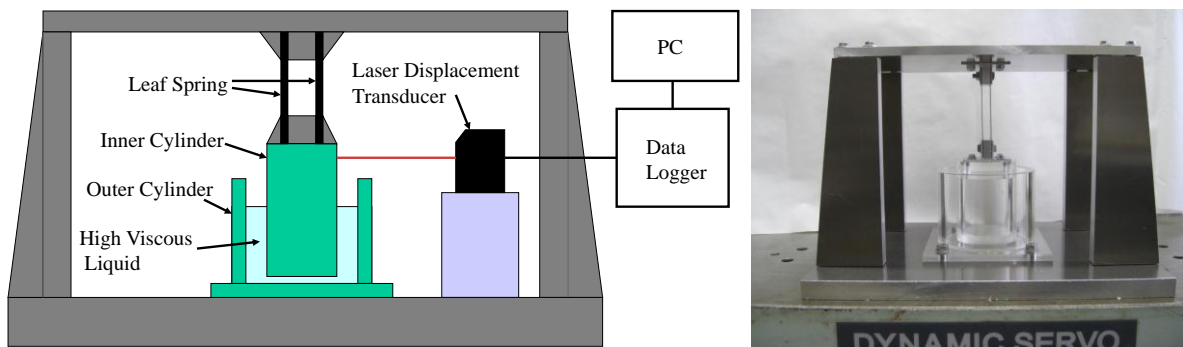


**Fig. 4.1.** Test Apparatus and Photo for Measuring Added Damping Coefficient
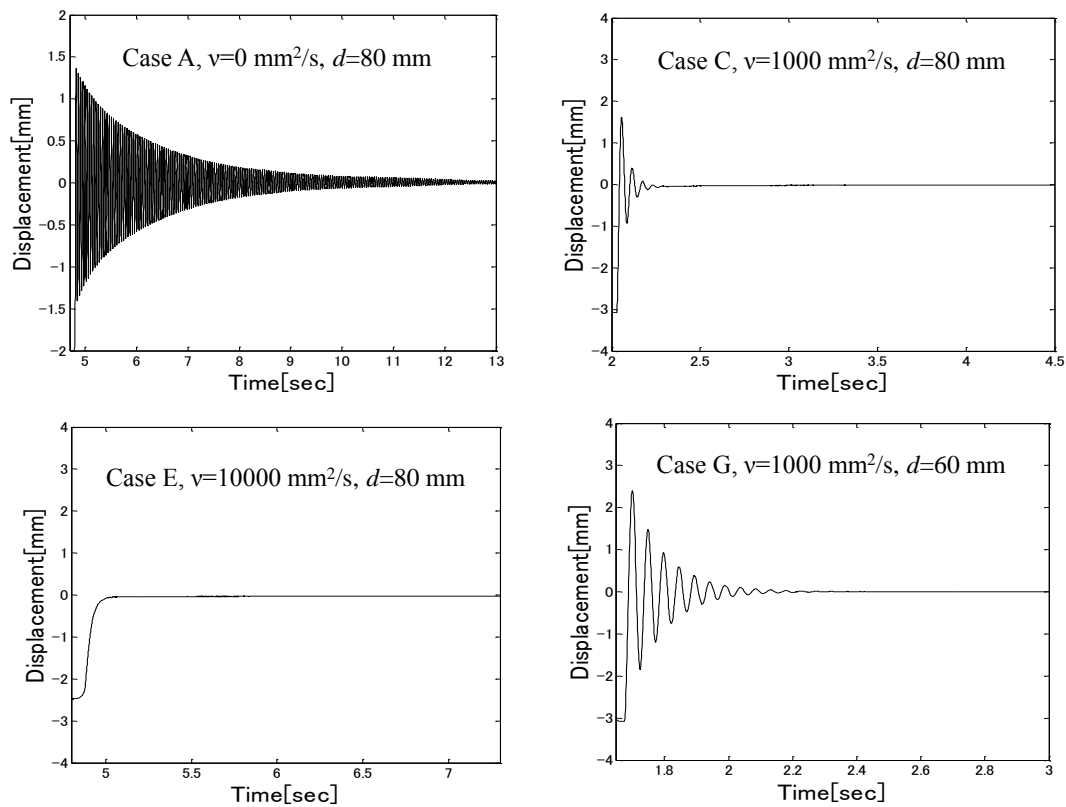


**Fig. 4.2.** Time Histories of Free Vibration for Various Kinematic Coefficient of Viscosity and $d/D$

obtained. Figure 4.3 illustrates the relationship between liquid viscosity and added damping coefficient $C_a$ and Fig. 4.4 shows the relationship between diameter ratio and added damping coefficient. It is known that damping coefficient increases almost linearly against the viscosity increase and also shows very steep increase as $d/D$ approaches to 1. These trends are consistent with the analytical results shown by Chen.
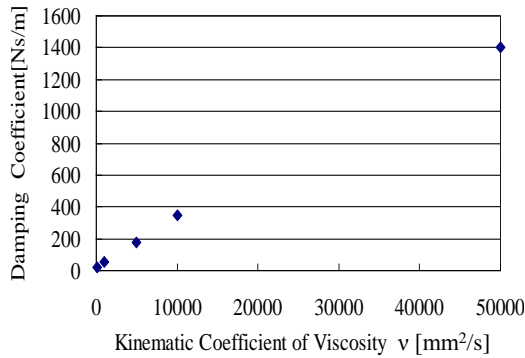


**Fig.4.3.** Added Damping Coefficient for Various Kinematic Coefficient of Viscosity
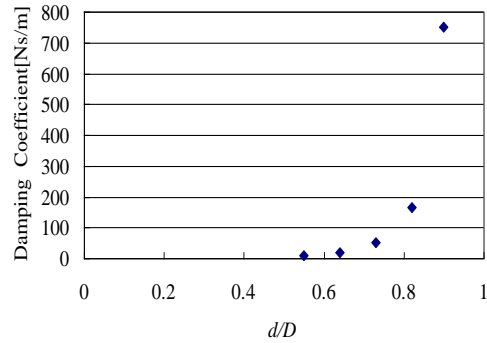
**Fig. 4.4.** Added Damping Coefficient for Various $d/D$

## 5. BASE ISOLATION TESTS AND ANALISIS

### 5.1. Test Apparatus

Simple sliding base isolation system is fabricated using the coaxial circular with the same dimensions used in the previous chapter. Figure 5.1 shows the outline of the test apparatus and top view. Upper structure is a square plate with 6 kg mass, 360 mm length and 10 mm thickness made of aluminium. 4 sets of coaxial circular cylinder systems are attached under the upper structure. The inner cylinders will slide at the top surface of the outer cylinder. Thin plastic plates made of Teflon are attached at the top end of the outer cylinders in order to make the friction force stable. This apparatus is settled on the shaking table. Sinusoidal excitations are applied to the base isolation system and the displacement and acceleration responses of the upper structure are measured. As well as in the damping coefficient tests, displacement is measured by a laser-type displacement transducer, while acceleration is measured by acceleration transducers. Before conducting sliding tests, friction coefficient is measured. Static and dynamic friction coefficients are 0.2 and 0.1 respectively. Test conditions for the cylinder diameter and the liquid viscosity are the same as shown in Table 4.1. Excitation frequency is 3 Hz and excitation amplitude is 10mm for all test cases.
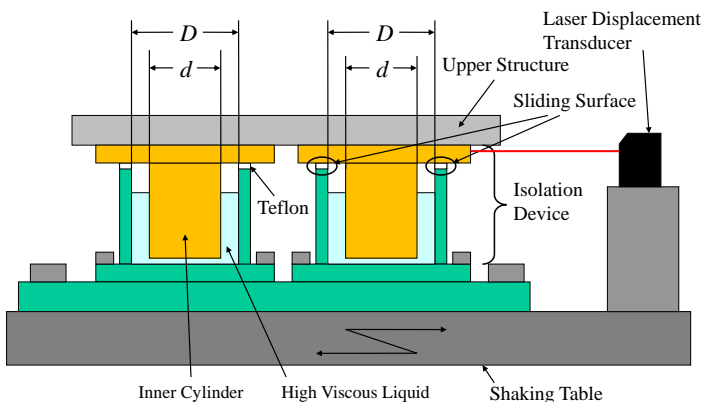


**Fig. 5.1.** Test Apparatus and Top View for Sliding Base Isolation Test by Shaking Table

## 5.1. Test Results

Displacement time histories and acceleration time histories for case A, C and E are shown in Figs. 5.2. It is noted that sliding displacement becomes small when we increase liquid viscosity while acceleration tends to increase for large liquid viscosity. Sliding displacements and accelerations for various liquid viscosities and diameter ratio $d/D$ are plotted in Figs. 5.3 and 5.4. It is found that the sliding displacement tends to decrease and response acceleration tends to increase according to the increase in liquid viscosity and in $d/D$. These tendencies are the same as those observed in analytical results shown in Fig. 3.5. In order to minimize the sliding displacement and to avoid the collision of the cask with the adjacent cask, large liquid viscosity is preferable, however, in the view point of the integrity of the inner structures such as spent fuels or to suppress rocking motion, small liquid viscosity is preferable. Therefore, the optimum value exists in the liquid viscosity and diameter ratio $d/D$.

(a) Case A, $\nu = 0$ mm$^2$/s, $d = 80$ mm

(b) Case C, $\nu = 1000$ mm$^2$/s, $d = 80$ mm

(c) Case E, $\nu = 10000$ mm$^2$/s, $d = 80$ mm
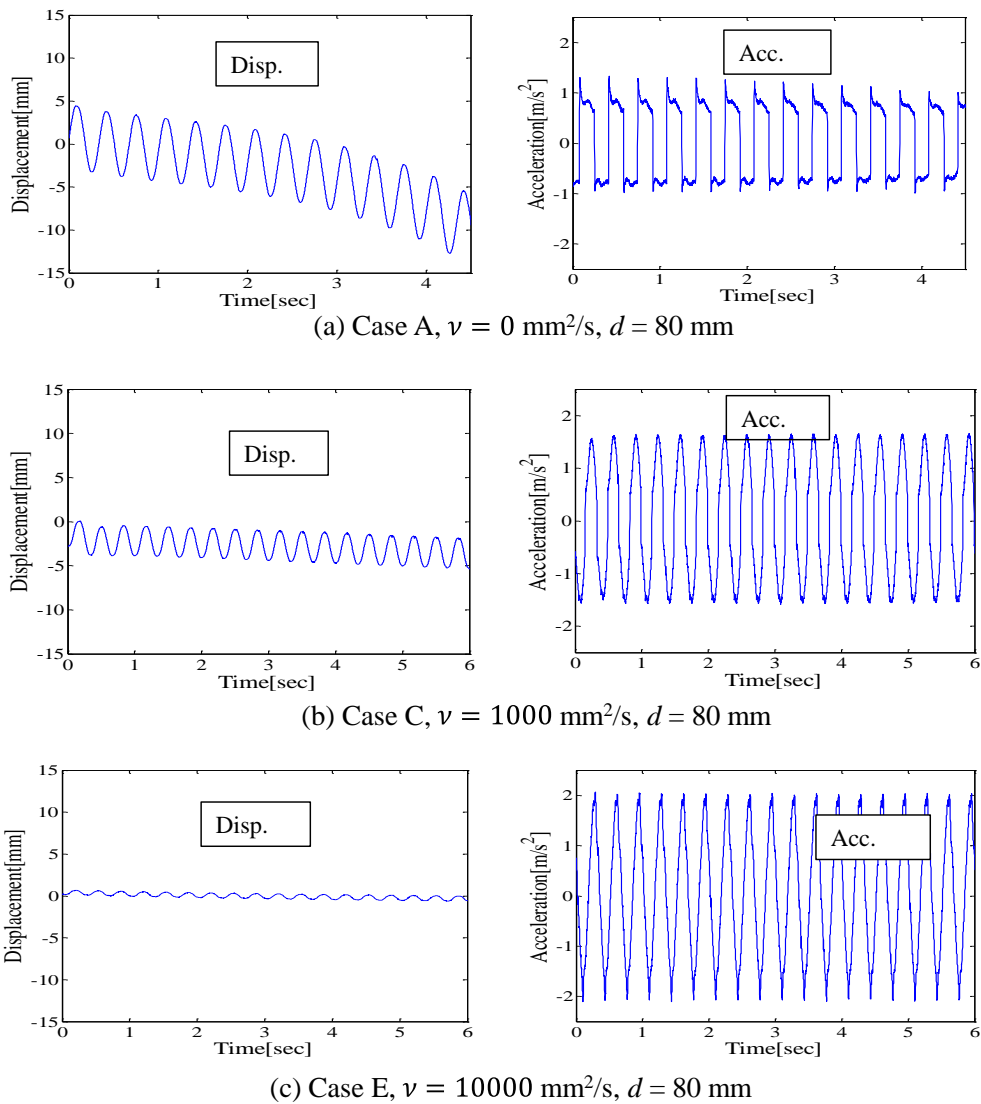
**Fig.5.2.** Measured Response Time Histories for Sinusoidal Excitation

## 6. CONCLUSIONS

A displacement suppression system applied to the cask-canister system which is a free-standing circular cylinder was proposed. This suppression system consists of a coaxial circular cylinders and
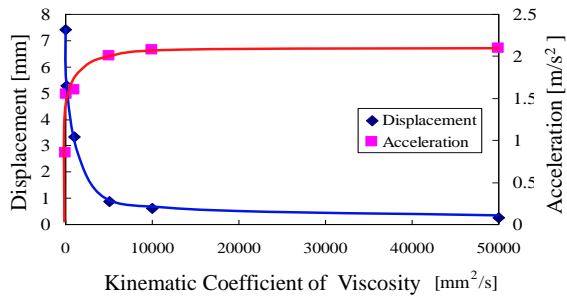
**Fig. 5.3.** Displacement and Acceleration for Various Liquid Viscosities
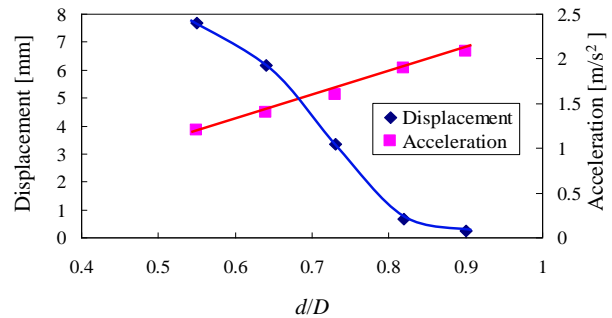


**Fig. 5.4.** Displacement and Acceleration for Various Diameter Ratios

viscous liquid installed in the annular space, and utilizing vary large added damping effects shown by Chen. On the other hand, from the view point of suppressing rocking motion and maintaining the structural integrity of the inner structure, the response acceleration should be minimized. The authors evaluated response displacement and acceleration of the cask system which has proposed sliding motion suppression devices analytically and experimentally.

In the analyses, response displacement and acceleration for the actual cask systems were evaluated for various damping coefficients. And it was confirmed that when damping coefficient increases, sliding displacement can be suppressed significantly, while response acceleration increases.

In the experiments, the authors fabricated a coaxial circular cylinder system and a fundamental sliding type base isolation system. Using these test apparatuses, the added damping coefficient for various liquid viscosities and d/$D$ ratios were measured. And using these coaxial circular cylinders, a fundamental sliding type base isolation system was fabricated and installed to the shaking table. Sinusoidal excitation tests were conducted and sliding displacement and response acceleration were measured for various liquid viscosities and diameter ratio d/$D$.

From these experimental and analytical results, it was confirmed that when we increase the liquid viscosity, sliding displacement can be suppressed significantly, however, response acceleration tends to increase. Therefore, it was concluded that in designing sliding suppression system proposed here, optimization is needed in liquid viscosity and diameter ratio d/$D$.

## REFERENCES

Chen, S.S., Wambsganss, M.W. and Jendrzejczyk, J.A. (1976). Added mass and damping of a vibrating rod in confined viscous fluids. *Journal of Applied Mechanics*. **16**, 325-329.

Furuta, K., Ito, T. and Shintani, A. (2009). A study on sliding motion of twe-degree-of-freedom coupled systems subected to seismic excitation. *Transaction of JSME C* **75:751**, 574-580.

Furuta, K., Ito, T. and Shintani, A. (2008). Fundamental study on sliding motions of two-degree-of-freedom coupled systems ab¥nd rocking motion of a rigid body. *Journal of System Design and Dynamics of the JSME* **2:1**, 36-44.

Furuta, K., Ito, T. and Shintani, A. (2008). A study on rocking phenomena of two-degree-of-freedom coupled systems subjected to base excitation. *Transaction of JSME C* **74:741**, 1093-1098.

Furuta, K., Ito, T. and Shintani, A. (2008). Study on the influence of a inner structure on sliding and rocking motions of a dual structure subjected to base excitation. *Journal of the Japan Association for Earthquake Enginnering* **8:3**, 31-45.

Central Research Institute of Electric Power Industry (2006). *CRIEPI Review* **52**, .

Shenton, H.W. and Jones, N.P. (1991). Base excitations of rigid bodies 1: Formulation. *Journal of Engineering Mechanics* **117**, 2286-2306.